Published in the Russian Federation
European Researcher
Has been issued since 2010.
ISSN 2219-8229
E-ISSN 2224-0136
Vol. 73, No. 4-2, pp. 720-735, 2014

DOI: 10.13187/issn.2219-8229
www.erjournal.ru

Physico-mathematical Sciences

Физико-математические науки

UDC 614.876

Statistical and Structural Properties of Radionuclide Deposition

Andry Grubich

CJSC TIMET, Belarus
Fabriciusa street 8, 220007, Minsk
Ph.D. (Phys. – Math.), Leading Researcher
E-mail: timet@inbox.ru

Abstract. The statistical properties of spatial patterns of radionuclide deposition are reviewed, making use of data for Chernobyl deposition of radionuclides ^{90}Sr, ^{137}Cs, ^{238}Pu, $^{239+240}$Pu, and ^{241}Am on sites and soil not cultivated after the accident. Examples considered in the article demonstrate how radionuclide deposition is described by the family of lognormal distributions that, along with multifractal spatial patterns of deposition, is an essential feature of their nature. Key results and conclusions of the article are applicable to the deposition of non-radioactive contaminating substances.

Keywords: Lognormal distribution; Mixture of lognormal distributions; Chernobyl and Fukushima fallouts.

Introduction

A number of works examined the distribution of radionuclide deposition can be described by lognormal distribution – see, in particular, the review of relevant articles in [1]. In [2], normal, Weibull, and lognormal distributions were fitted to 64 datasets for ^{90}Sr, ^{134}Cs, ^{137}Cs, ^{238}Pu, $^{239+240}$Pu, and ^{241}Am on sites with varied surface areas, and datasets with large sample size were shown to be best described by lognormal distributions in the vast majority of cases. For instance, out of 15 datasets of activity density (Bq/m^2) with sample size $n \geq 60$, there was only one that was not described by a lognormal distribution, i.e., the probability of data description by lognormal distribution proved to be equal to P=14/15=0.933. For activity concentrations (Bq/kg), all nine datasets with large sample size were described by lognormal distribution. These results suggest that the description of radionuclide deposition by the family of lognormal distributions is by no means a rare phenomenon but rather a regular occurrence that is an essential feature of the nature of the radionuclide deposition.

Any site can be divided into several sub-sites, and vice versa, several sub-sites can be aggregated into one site. The property of deposition lognormality implies that the radionuclide distribution on the site and the sub-sites that form it should be described by a family of lognormal distributions. From the mathematical point of view this means that a mixture of lognormal distributions for sub-sites, in its turn, is also a lognormal distribution. It is evident that this can be true only for the case of particular statistical and structural properties of radionuclide deposition. This article deals with the analysis of these properties.

The analysis performed is topical regarding the phenomenological explanation of radionuclide deposition lognormality. If subsequently the property of deposition lognormality obtains wide recognition in practice, it will open up new ways for the optimisation of radiation control and monitoring methods, including protection and remediation measures as topical issues.

Materials and Methods.

This article makes use of datasets described in [2]. Due to this, below is given only the information about sites and their radioactive contamination that was not published earlier. For convenience of data handling, the designations of sites and numbering of datasets introduced in [2] have been retained.

In [2], it was shown that the distributions of radionuclides ^{137}Cs, ^{238}Pu, and $^{239+240}$Pu on site P4 were formed by four sub-sites P4.1–4.4 (with areas of 8.5 km^2 each) and were best described by lognormal distributions $\Lambda(\mu, \sigma^2)$. Estimates of the numerical values of the lognormal distribution parameters for these radionuclides are listed in

Table **1** ($\mu \approx \mu_{fit}$, $\sigma \approx \sigma_{fit}$). The datasets of the ^{90}Sr and ^{241}Am on sub-sites P4.1, P4.3, and P4.4 were best described by Weibull distributions $W(\alpha, \beta)$. Estimates of the numerical values of the Weibull distribution parameters ($\alpha \approx \alpha_{fit}$, $\beta \approx \beta_{fit}$) for these sub-sites and the lognormal distributions for sub-site P4.2 and site P4 are given in Table 1.

Table 1: Parameters[a] of the lognormal and Weibull distributions.

Nuclide	Site	Dataset	μ_{fit} [b]	σ_{fit}	α_{fit}	β_{fit} [b]
^{137}Cs	P4.1	6	7.77	0.436	—	—
	P4.2	11	8.05	0.505	—	—
	P4.3	16	8.24	0.352	—	—
	P4.4	21	8.34	0.354	—	—
	P4	26	8.10	0.468	—	—
^{90}Sr	P4.1	7	—	—	2.16	346
	P4.2	12	5.54	0.663	—	—
	P4.3	17	—	—	2.22	408
	P4.4	22	—	—	1.56	537
	P4	27	5.70	0.675	—	—
^{241}Am	P4.1	8	—	—	2.96	16.6
	P4.2	13	2.27	0.384	—	—
	P4.3	18	—	—	3.41	13.1
	P4.4	23	—	—	2.89	22.4
	P4	28	2.55	0.472	—	—
^{238}Pu	P4.1	9	0.980	0.592	—	—
	P4.2	14	0.866	0.378	—	—
	P4.3	19	1.09	0.367	—	—
	P4.4	24	1.30	0.510	—	—
	P4	29	1.06	0.493	—	—
$^{239+240}$Pu	P4.1	10	1.74	0.571	—	—
	P4.2	15	1.62	0.377	—	—
	P4.3	20	1.85	0.375	—	—
	P4.4	25	2.06	0.499	—	—
	P4	30	1.82	0.489	—	—

[a]Methods estimates of parameters were described in Grubich et al. (2013).
[b] For activity density (kBq m^{-2}).

This article also uses data on the contamination of site B1, 50 m x 50 m with coordinates 26°68´59.3´´ E и 53°94´63.8´´ N. Parameters of the lognormal $\Lambda(\mu, \sigma^2)$ and normal $N(\mu, \sigma^2)$ distributions best described the contaminations of site B1 by ^{137}Cs as a whole, and four zones marked on its surface (see below) are given in
Table 2.

Table 2: Parameters of the lognormal and normal distributions.

Zone or site	$\Lambda(\mu, \sigma^2)$		$N(\mu, \sigma^2)$	
	μ_{fit}[a]	σ_{fit}	μ_{fit}[a]	σ_{fit}
Zone 1	—	—	81.0	16.0
Zone 2	—	—	79.3	20.5
Zone 3	4.47	0.334	—	—
Zone 4	4.34	0.227	—	—
B1	4.38	0.267	—	—

[a] For activity density (kBq m^{-2}).

Datasets for Chernobyl fallout reviewed in the article were derived using a two-dimensional systematic grid sampling. In this case, the dataset is

$$x_1(r_1), x_2(r_2), \ldots, x_n(r_n), \quad (1)$$

where $x_i = x_i(\mathbf{r}_i)$ – activity density (kBq/m²); $\mathbf{r}_i$ – vector defining position of the i^{th} sampling point on the site surface divided into n equidimensional blocks.

Sample (1) contains information on the spatial pattern of radionuclide deposition on the site and is of interest for the analysis of multifractal [3] and geostatistical properties of depositions used in contamination mapping [4]. This article, similar to previous reviews [5] and [2], considers solely the statistical properties of the datasets; therefore, information about the coordinates of sampling points in (1) is omitted

$$x_1, x_2, \ldots, x_n, \quad (2)$$

and dataset (2) is considered.

It should be noted that (1) and (2) are the same set of scalar quantities.

Datasets can be derived for several sub-sites located as shown, for example, in Figure 1a. The dataset for all sub-sites combined can be derived by simple addition of the datasets of the sub-sites. Next, one can seek the distribution F(x) that best describes the empirical distribution $F_n(x)$ derived for the resulting dataset. This method was used in [2] for the analysis of types of distributions that describe datasets for sub-sites P4.1–4.4 and site P4 formed by the combination thereof.

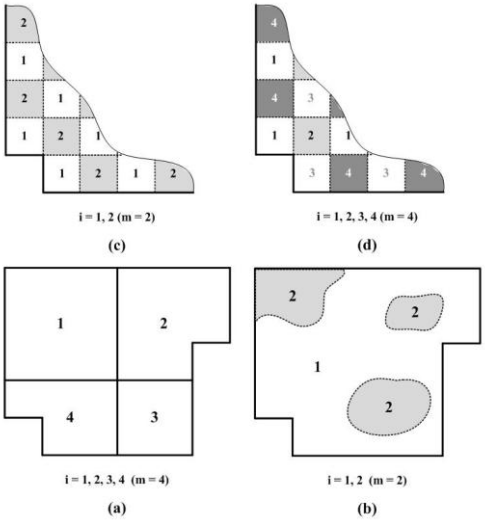

Figure 1. Example of location: (a) – neighbouring sub-sites (1–4); (b) and (c) – zones (1, 2); (d) – zones (1–4).

The alternative method consists in summing up distributions derived for each of the sub-sites:

$$F(x) = \sum_{i=1}^{m} w_i F_i(x), \quad (3)$$

where F(x) –distribution function (cumulative distribution function) of the mixture distributions for m sub-sites; w_i – weight coefficients satisfying condition

$$\sum_{i=1}^{m} w_i = 1; \quad (4)$$

$F_i(x)$ – distribution function for i^{th} sub-site.

In the general, the case weight the coefficients in (3) are equal

$$w_i = S_i/S, \quad (5)$$

where S_i – surface area of the i^{th} sub-site; S – total surface area of all sub-sites.

Instead of (3), the mixture of the probability density functions

$$dF(x)/dx = \sum_{i=1}^{m} w_i \, dF_i(x)/dx_i \quad (6)$$

can be used.

The mixture of distributions (6) can also be used in the case of datasets for several zones singled out on any site. Assume that a site with the diagram shown in Figure 1b was investigated, and two datasets were derived as a result. If $F_i(x)$ is the distribution function for the i^{th} zone (in this example i = 1, 2), then the mixture of distributions (6) describes the distribution for the site as a whole. In cases such as these, in (5), the quantity S_i is equal to the surface area of the i^{th} zone. It is reasonable to use the pattern of site division, given in Figure 1b, for analysis of the statistical characteristics of site regions having varied landscape characteristics or some other important feature. For example, the area of site P4 is 34 km² (4 x 8.5 km²). Approximately 70% of the surface of site P4 is wooded. Datasets for each of the radionuclides on site P4 can be broken up into two datasets, with one of them corresponding only to open sections of the site (from now on called – "field" zone) and the other to wooded site sections (from now on called – "wood" zone).

The site division into zones (or dataset division into sub-sites, corresponding to zones) can also be used for evaluation of the probability of the description of site contamination by any given type of distribution with the increase of the sample size. Thus, the example of site division into zones is shown in Figure 1c. In this example, two zones are formed by different groups of square grid blocks. Below an example is considered with a more complicated pattern of site B1 division into four zones (see Figure 1d). In all cases such as these, weight coefficients are equal to

$$w_i = 1/N_i, \quad (7)$$

where N_i – number of grid blocks with index i.

Discussion.

As stated in the introduction, the result of deposition lognormality is that a mixture of lognormal distributions for sub-sites describing deposition distribution on the aggregated site,

$$dF(x)/dx = \sum_{i=1}^{m} w_i d\Lambda_i(x|\mu_i, \sigma_i^2)/dx \quad (8)$$

should be a lognormal distribution.

Daniels and Higgins while considering radioactive contamination of various objects, concluded that an assumption of lognormality is an idealisation [1]. However, this should not be considered a limitation of the lognormal model.

Indeed, in the general case, a mixture (8) can only approximately be a lognormal distribution (for example, in the case of m = 2 and $\mu_1 \neq \mu_2$ or/and $\sigma_1 \neq \sigma_2$). Moreover, from the empirical point of view (in the case where properties of finite datasets are considered jointly with the results of actual measurements), the property of deposition lognormality implies that contamination of any site in the general case is described by a lognormal distribution only approximately. Still, even for an approximate description of a mixture (8) by lognormal distribution, certain conditions should be satisfied. For example, the condition that the parameters of lognormal distributions μ_i and σ_i for all mixture components have close numerical values.

Figure 2a shows the dependence of values of the sample standard deviation, s, on the sample mean, x_o, for radionuclide deposition on neighbouring sub-sites P4.1-4.4, as per the data in Table 1a in [2]. Note that these sub-sites are located relative to each other in a way similar to the sub-sites in Figure 1a. Unlike the sub-sites in Figure 1a, sub-sites P4.1-4.4 have a somewhat different external outline and the same surface area: 8.5 km² each. For different radionuclides, points (x_o, s) are designated in Figure 2a by different geometric figures. For comparison Figure 2a, also shows

points (x_0, s) in the case of the division of site B1 into zones according to pattern in Figure 1d. Note that points for zones 2 and 4 in Figure 2a overlap.

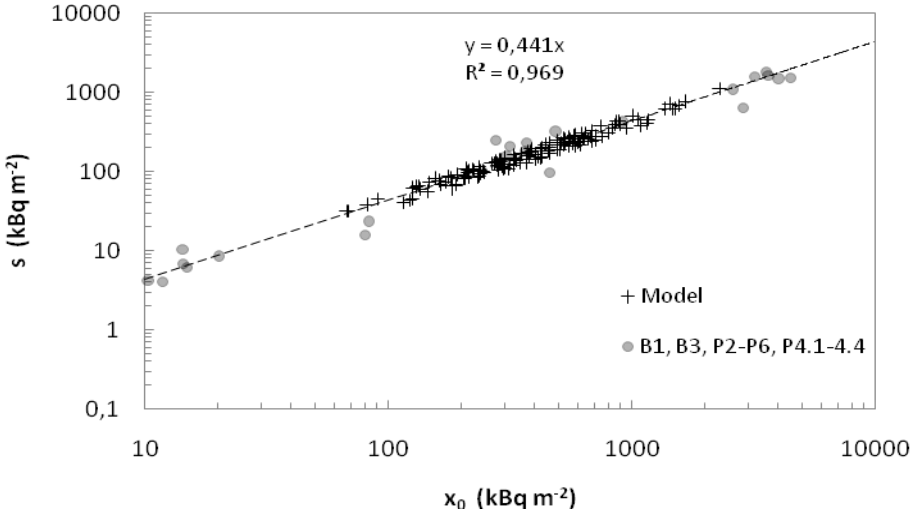

(c)

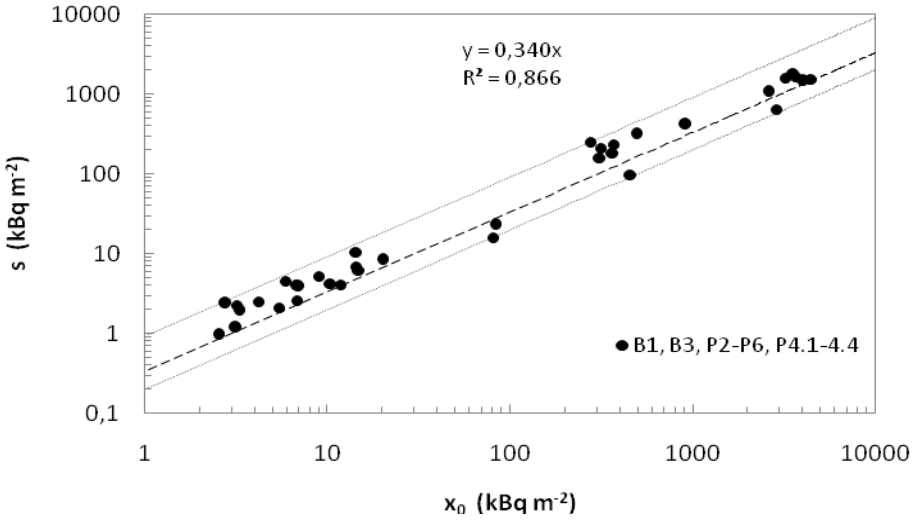

(b)

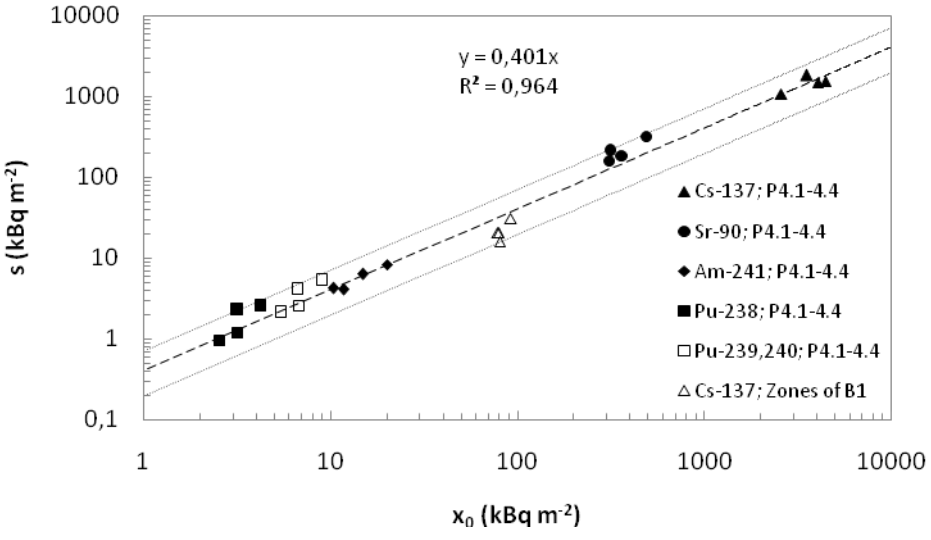

(a)

Figure 2. Values of standard deviations against the sample mean x_0: (a) – for neighbouring

sub-sites P4.1–4.4 and zones on site B1; (b) – for data in Table 1a in Grubich et al. (2013); (c) – for the results of the model considered in subsection 4.4.1, crosses.

The linear regression equation (dotted line) corresponds to the entire aggregate of points shown in the figure. Regions where points (x_o, s) are scattered have the shape of the band formed by two lines. These boundaries pass through the point corresponding to data for ^{137}Cs on site B1, zone 1 (bottom boundary), and the point for ^{238}Pu on sub-site P4.1 (top boundary).

For each of the radionuclides, the points (x_o, s) in plot of Figure 2a formed a concentrated cloud. Due to this fact, a mixture (8) corresponding to each of the point clouds (x_o, s) is approximately described by a lognormal distribution. A number of examples will demonstrate this below.

Figure 3a and Figure 3b show examples of mixtures for site P4 with all components belonging to an aggregate of lognormal distributions: a mixture for distributions of ^{137}Cs on sub-sites P4.1–4.4; a mixture for distributions of ^{137}Cs on zones “field” and “wood” of site P4. In addition to the mixture and its components in Figure 3a and Figure 3b, the heavy dotted line shows the function of the lognormal distribution probability density, which is the best way to describe the dataset for ^{137}Cs on site P4 (distribution parameters of μ_{fit} and σ_{fit} as per

Table **1**). Both mixtures are adequately described by a lognormal distribution. Similar results are obtained for distributions of ^{238}Pu and $^{239+240}$Pu on sub-sites P4.1–4.4.

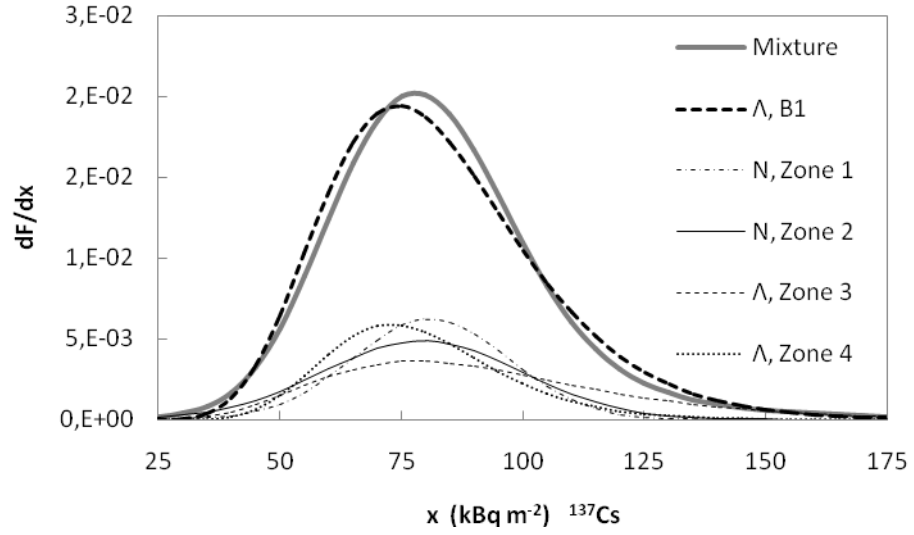

(d)

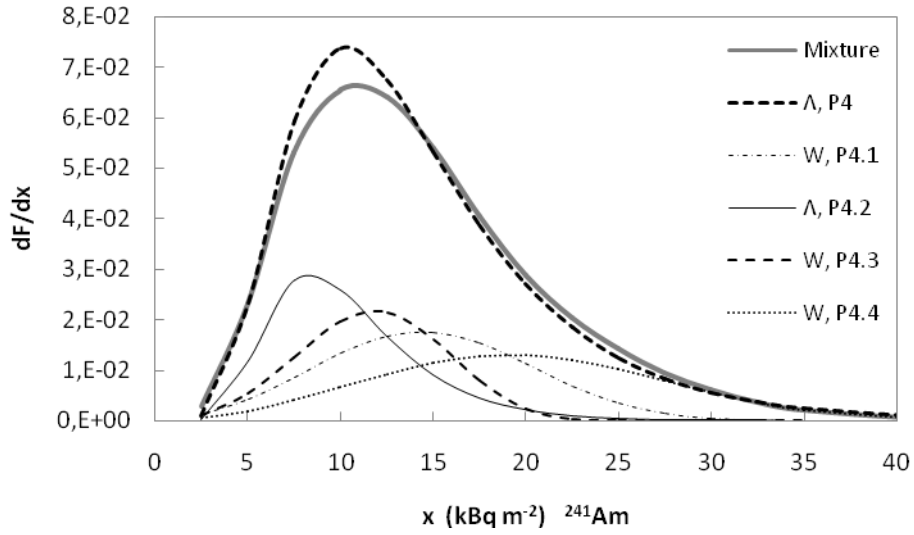

(c)

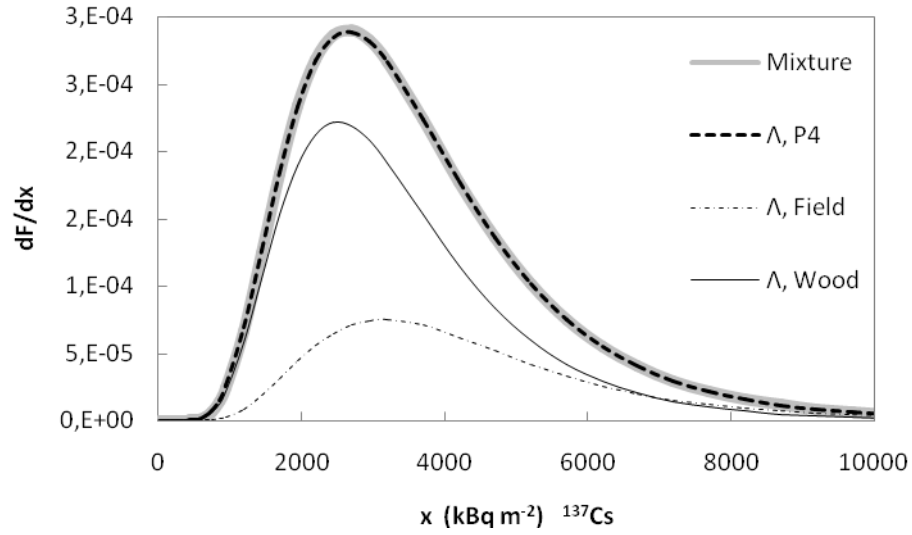

(b)

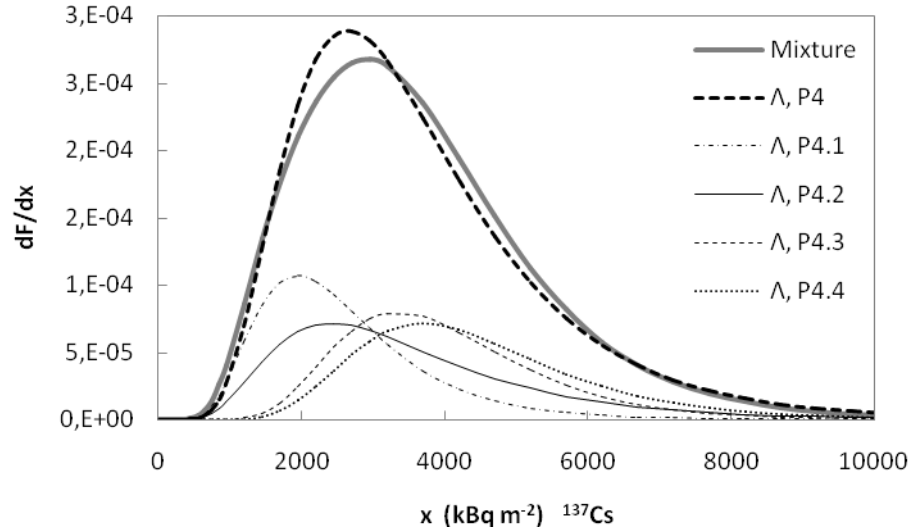

(a)

Figure 3. Mixture of the probability density functions: (a) – ^{137}Cs on sub-sites P4.1–4.4; (b) – ^{137}Cs for two zones on site P4; (d) – ^{241}Am on sub-sites P4.1–4.4; (c) – ^{137}Cs for four zones on site B1.

In all cited examples, the description of mixtures by lognormal distributions is explained by the fact that points (x_o, s) for sub-sites (or zones) are located close one to another, see, in particular, Figure 2a. As a result, the parameters of lognormal distributions of varied mixture components also have similar values.

Indeed, the parameters of the lognormal distribution describing the dataset can be derived by the method of moments [6]. In this case, estimates of the parameters of the lognormal distribution that describe the dataset with sample values of x_o and s, are equal to:

$$\mu = \ln x_0 - \sigma^2/2, \quad (9)$$

$$\sigma = [\ln(1 + CV^2)]^{1/2}, \quad (10)$$

where $CV = s/x_o$ – is the coefficient of variation.

Thus, the lesser the scattering of points (x_o, s) is for datasets of neighbouring sub-sites (or for zones on one and the same site), the lesser scattering of corresponding points (μ, σ) is for the parameters of the lognormal distributions. If however, any of the mixture components (8) still varies from the remaining ones (as, for example, the distribution density function for sub-site P4.1

in Figure 3a), then for the case of a large number of mixture components, this is not so conspicuous. As a result, the mixture (8) is approximately described by a lognormal distribution.

In practice, the property of deposition lognormality is dominant only in the case when datasets with large sample sizes are used. If the sample size is small (as, for example, in the case of sub-sites P4.1–4.4 with n = 33 or 34), then datasets are often described by distributions different from lognormal.

As it was mentioned above, aggregation of datasets for neighbouring sites (or zones) may be collated by a mixture of distributions that describe these datasets. Therefore, the analysis of mixtures of different aggregates makes it possible, on the one hand, to determine conditions under which such a mixture is a lognormal distribution and, on the other hand, evaluate the sample size starting from which datasets are, as a rule, described only by lognormal distributions.

Figure 3c and Figure 3d show mixtures for the depositions of ^{241}Am on sub-sites P4.1–4.4 and for the deposition of ^{137}Cs on site B1 (in the case of division of site B1 into four zones according to a pattern similar to the one given in Figure 1d). The normal, Weibull and lognormal distributions are denoted in the figures by the letters N, W and Λ, respectively. Lognormal distributions are the best way for describing the datasets for ^{241}Am on site P4 and ^{137}Cs on site B1 and are shown in Figure 3c and Figure 3d by heavy dotted curves. As observed from these examples, mixtures of distributions of varied aggregates (Weibull and lognormal distributions – Figure 3c; normal and lognormal distributions – Figure 3d) are also adequately described by lognormal distributions. It can be shown that a similar result is also obtained for deposits of ^{90}Sr on sub-sites P4.1–4.4.

In last three examples the reasons for describing the mixture by lognormal distributions are not as evident as for the cases considered above. However, the given examples have a number of common features.

A. Sample points (x_o, s) for the mixture components, as in the examples given above are spaced closely one to another – see plot in Figure 2a.

B. Sub-sites (or zones on a site) can be mutually summed up by twos, threes, etc. In this connection, one may show that for each of the examples considered in this sub-section, the following holds. Once one of the components of the two-component mixture is found to be a lognormal distribution, such a mixture, in turn, is best described by a lognormal distribution. The same holds for the above-given examples in the case of all possible three-component mixtures.

On the basis of these features, one can assume that the mixture of distributions of varied aggregates corresponding to aggregated neighbouring sites (or aggregated zones of the site) is described by a lognormal distribution if condition A is satisfied and at least one of the mixture components is a lognormal distribution.

The last three examples make it possible to speak about the following regularity. If for small sampling sizes the dataset is described by a distribution different from lognormal (for example, normal or Weibull distribution), with sampling sizes n ≥ 100, the dataset will overwhelmingly be best described by a lognormal distribution.

Indeed, in the case of the distribution of ^{241}Am on sub-sites P4.1–4.4 (Figure 3c), for all possible mixtures having various numbers of components, with the increase of the number of components from m=2 to m=4, the probability of describing the mixture by a lognormal distribution increases and becomes equal to one in the case of the addition of all four components. The same is true for the distribution of ^{90}Sr on sub-sites P4.1–4.4. For all possible mixtures of the distribution of ^{137}Cs on site B1 (Figure 3d), the probability becomes equal to one in the case of the addition of any three components because in such mixtures (m = 3), there is sure to be a component described by a lognormal distribution. Datasets that correspond to such mixtures have the following sample sizes: n = 136 for ^{241}Am, n = 134 for ^{90}Sr and n = 75 for ^{137}Cs. On the basis of these examples, as an evaluation of the empiric dataset sample size, starting from which the property of a lognormal deposition starts to display itself in practice, one may take the value n = 100.

Note that sample size can be increased either by taking additional measurements on the site (for example, a mixture of distributions for zones on site B1) or by combining datasets for two or more neighbouring sites into a single dataset (for example, a mixture of distributions for sub-sites on site P4).

Let us assume that an arbitrary territory is divided into m equal-sized sub-sites, and the quantity m >> 1. Because m >> 1, then in this case, the totality of sub-sites under consideration has

sub-sites significantly remote from each other. Hence, the mean values for the sub-sites can, in principle, noticeably vary. Let us also assume that the sample values of the mean, x_{oi}, and standard deviations, s_i, for each sub-site are known (i = 1, 2, ..., m). In this case, points (x_{oi}, s_i) will be scattered on the plot similar to the plot in Figure 2a.

Really, in Figure 2b, black circles show the points (x_{oi}, s_i) for all 35 datasets of Table 1a in [5]. It is a reminder that these datasets correspond to the deposition of different radionuclides (^{90}Sr, ^{137}Cs, ^{238}Pu, $^{239+240}$Pu, and ^{241}Am) on 11 sites (including sub-sites P4.1–4.4), with variation of site area from 1.56 m^2 to 1.42·10^8 m^2. Figure 2b also cites a linear regression equation (dashed straight line) derived for all points shown in the figure.

As can also be observed in this case, the vast majority of points (x_o, s) are scattered across a band-shaped region, which however turned out to be somewhat wider than the band in Figure 2a plotted for neighbouring sub-sites. The lower boundary of the band in Figure 2b

$$s = CV_{min} \cdot x_o \quad (11)$$

passes through point (x_o, s) corresponding to the dataset for tiny site B3 with a surface area of only 1.56 m^2, located approximately 370 km away from the Chernobyl Nuclear Power Plant (CV_{min} = 0.201).

The upper boundary

$$s = CV_{max} \cdot x_o \quad (12)$$

passes through point (x_o, s) corresponding to the dataset for ^{90}Sr on site P3, having a surface area of 1.42·10^8 m^2 and located approximately 20 km away from Chernobyl Nuclear Power Plant (CV_{max} = 0.912).

To avoid possible misunderstandings, one has to note that the region where points (x_o, s) are scattered is band-shaped only on the plot with logarithmic scales on both axes. On a plot with linear scales of axes, the relevant region will have the shape of sector formed by two beams (11) and (12) starting from the origin of the coordinates.

With regard to the pattern of the scattering of points (x_o, s) in Figure 2b and great variety of sites that correspond to them (in the context of the sites' surface area – from 1.56 m^2 to 1.42·10^8 m^2 – and their location in different regions of Belarus), one may assume that on the log-log plot for the multiplicity of sub-sites on any contaminated territory, the points (x_{oi}, s_i) will also be scattered across the region in the shape of a band arranged along the linear regression equation $s = b \cdot x_o$ with values $b \in [CV_{min}, CV_{max}]$.

The form of the lognormal distribution plot determined by the numerical value of the form parameter, σ. According to (10), the numerical value of the form parameter depends on the sample coefficient of variation, CV. For sites with surface areas from 1.56 m^2 to 1.42·10^8 m^2, values of CV, as shown in sub-section 4.3.2, are contained in interval $[CV_{min}, CV_{max}]$, to which the interval of values of σ from σ_{min} = 0.199 to σ_{max} = 0.778 correspond.

The scale parameter, μ, determines the position of the median, med, of the distribution of $\Lambda(x|\mu, \sigma^2)$ on axis X. Therefore, forms of the lognormal distribution plot having various values of scale parameter, μ, are convenient to be mutually collated using instead of the argument x magnitude t = x/med. Figure 4 shows the functions of the probability density of the lognormal distribution for variable t (i.e., for any μ) had numerical values of σ_{min} and σ_{max}. Therefore, for sites having surface areas in the range from 1.56 m^2 to 1.42·10^8 m^2, the multiplicity of all possible forms of the probability density function, which describes the deposition (in particular, all distributions corresponding to points (x_o, s) in Figure 2b), are enclosed between two "extreme" distributions, as shown in Figure 4.

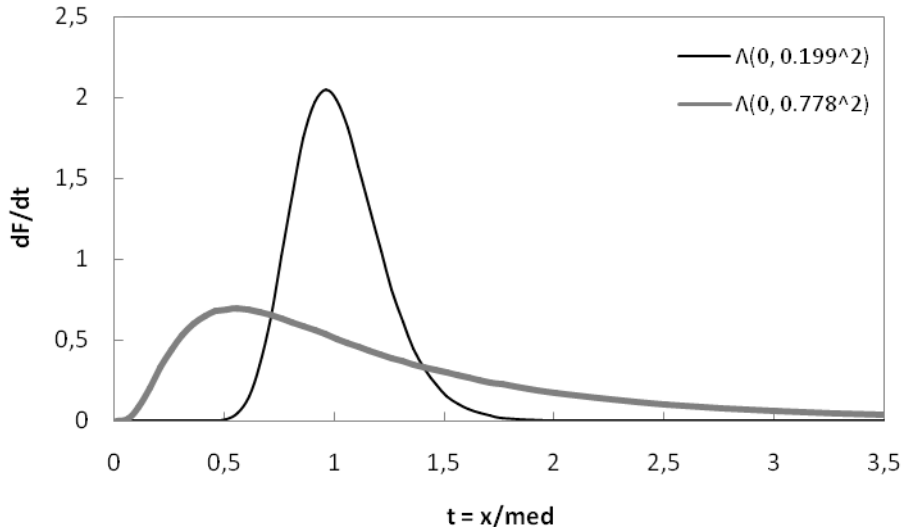

Figure 4. Forms of "extreme" probability density functions.

The linear regression for the standard deviation value from the mean described above implies that regression dependence of the coefficient of variation from the mean is not. Consequently, in the case of breaking up an arbitrary site/territory into a multiplicity of equidimensional sub-sites, the value of the coefficient of variation for the i^{th} sub-site

$$CV_i = s_i/x_{oi} \quad (13)$$

belongs to some interval $[CV_a, CV_b]$, whose width does not depend on the value of the mean, x_{oi}. Thereby, the values of CV_i are randomly distributed in the interval $[CV_a, CV_b]$ which, in turn, is included in the interval approximately equal to [0.2, 0.9] (see (11) and (12)).

If any site is divided into a large number of sub-sites, then the mean values of the contamination of the sub-sites

$$x_{o1}, x_{o2}, \ldots, x_{om} \quad (14)$$

will be best described by a lognormal distribution

$$\Lambda = \Lambda(x_o|\mu_o, \sigma_o^2). \quad (15)$$

From one site to another, only the parameters of the lognormal distribution, μ_o and σ_o, change.

For example, at sites P2 and P3, the areas of the square grid block equal 1 km^2. The method used to determine the magnitude of contamination of each of the blocks of site P3 was described in subsection 2.1 in [2]. This same method was also used for site P2. The value of x_i determined for the i^{th} block and included in dataset (2) is a rough estimate of the mean x_{oi} for this block (or, in other words, for this sub-site) and, in principle, could have been determined more accurately, for example, by dividing the block (sub-site) into a multiplicity of sub-blocks (sub-sub-sites), evaluating the contamination of each of them and then computing the mean.

The statistical properties of radioactive deposition described above can be used for building a model of the deposition on the site, where the mean contamination values of the individual sub-sites differ greatly.

Consider a hypothetical example of a vast territory broken up into 144 sub-sites (m = 144). Let us assume the values of the lognormal distribution parameters (15) as $\mu_o = 6$ and $\sigma_o = 0.75$. For the sake of simplicity, we will further assume that the values of the variation coefficients for the sub-sites (13) are evenly distributed within the interval [0.350, 0.514] – the interval of the values of the CV_i for ^{137}Cs on sub-sites P4.1–4.4. One may demonstrate that the mixture obtained later for m = 144 does not practically depend on the selected width of the interval of the CV_i values.

By using these assumptions and a random number generator, one may develop m values of quantities x_{oi} and CV_i (i = 1, 2, …, m). The derived results ($s_i = x_{oi} \cdot CV_i$) are shown in Figure 2c and Figure 5 by crosses – Model. For comparison, Figure 2c and Figure 5 also show scatter of points (x_{oi} s_i) and (x_{oi}, CV_i) – circles – for the data of Table 1a in [2].

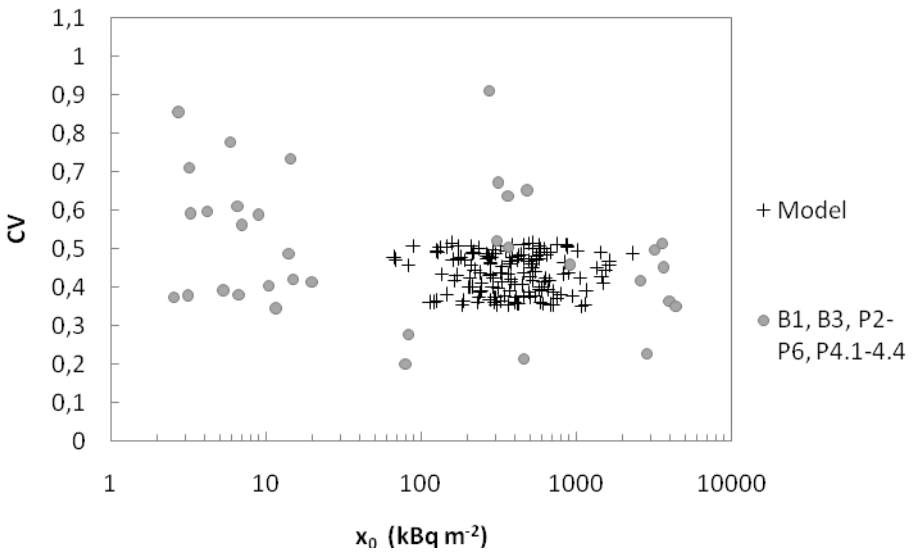

Figure 5. Values of the coefficient of variation CV against the sample mean x_o.

Let us then calculate the parameters of the lognormal distributions $\Lambda_i(x|\mu_i, \sigma_i^2)$ that describe the distribution of deposition on the hypothetic sub-sites under consideration. To this end, one may use, for example, formulae (9) and (10), substituting into them the simulated results of the values of CV_i and x_{oi}. The mixture (8) of the derived lognormal distributions is shown in Figure 6a by the thick grey curve. The dashed-line curve in Figure 6a shows the result of fitting a lognormal distribution to the derived mixture.

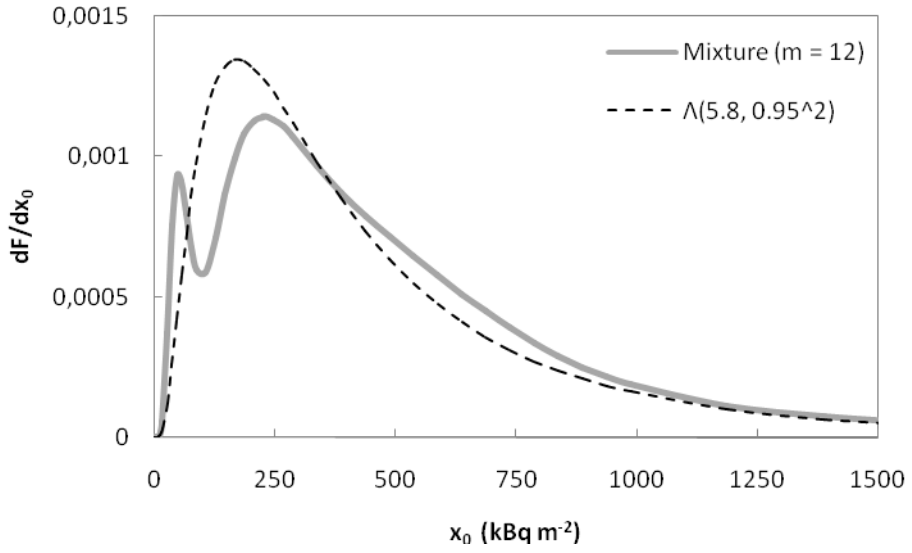

(b)

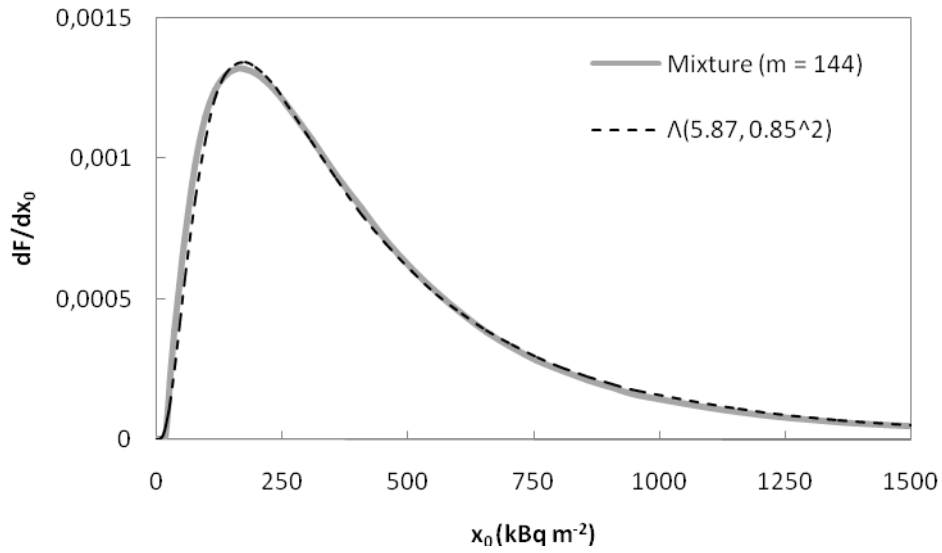

(a)

Figure 6. Mixture of the probability density functions simulating the distribution of deposition over a vast territory: (a) – m = 144, (b) – m = 12.

As observed, the derived mixture is adequately described by the lognormal distribution. The minimal and maximal mean values of the activity density for the sub-sites were 67.9 kBq/m² and 2309 kBq/m² (or 1.8 Ci/km² and 62 Ci/km²). If the number of sub-sites is not large, the mixture is not described by a lognormal distribution. Thus, Figure 6b cites the results derived for the considered model at m = 12.

The example considered above shows that on the territory, where the mean values of the activity density on the sub-sites differ by more than three hundred times, the distributions of deposition both on the territory as a whole and on the sub-sites that compose it, can be described by the family of lognormal distributions. To this end, it is necessary that the number of sub-sites was sufficiently large, and the contamination of each sub-site was described by a lognormal distribution. However, these conditions can be satisfied for any large site (territory).

Indeed, contaminations of tiny sites with areas from one and a half square meters and larger are described by a lognormal distribution – see, for example, sites B1, B3, P5, and P6 in Table 1a in [5]. The pollution levels of the closely spaced sites do not differ much. The coefficients of variation for the sites are distributed within a relatively narrow interval of values $[CV_a, CV_b]$. As a consequence, the parameters of the lognormal distributions, $\Lambda_i(x|\mu_i, \sigma_i^2)$, that describe the contamination of these sites do not differ much either. As a result, the mixture of distributions of (8) for such sites is also described by a lognormal distribution. Hence, in the case of a stage-by-stage division of a vast site (territory) into sub-sites, we finally find that the contamination of each sub-site is described by a lognormal distribution. In other words, each small area of spatial contamination pattern of some site/territory has a corresponding lognormal distribution, and the contamination of the site/territory as a whole is described by a mixture of these distributions, which, in turn, is also a lognormal distribution.

The minimal surface of such areas by order of magnitude is likely to be no more than 1 m² – see [5]. One can also assume that the property of contamination lognormality of such small areas is caused by air turbulence near the surface of the earth. On the other hand, due to horizontal (lateral) diffusion of radionuclides in soil for old fallouts (existing for at least dozens of years), the surface of such areas cannot be smaller than 1 m².

For illustrative purposes of how the described model is applied, let us consider a hypothetical example of a site on which in zone 1 the deposition is formed by dry fallout and in zone 2 by wet fallout. The zones can be spaced, for example, as shown schematically in Figure 1b. For definiteness let us assume the following. The areas of both zones are equal, and each zone is divided into 72 equidimensional sub-sites.

Within the framework of the model under consideration, the site contaminated by both dry and wet fallout can be described by the means of two distributions (15) with different parameter values. So, for example, Figure 7 shows a mixture of two probability density functions for distributions (15) with the following parameters: $\mu_D = 3.50$, $\sigma_D = 0.472$ (dry fallout), $\mu_W = 5.51$, $\sigma_W = 0.472$ (wet fallout).

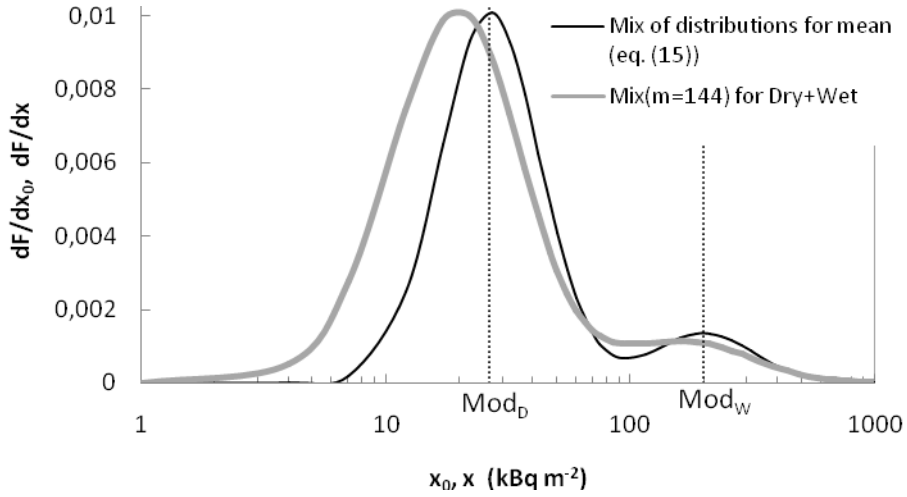

Figure 7. Mixture of the probability density functions simulating the distribution of dry and wet fallouts.

The derived mixture (fine line) has two maxima and, hence, is not a unimodal distribution. The modes of these two distributions are correspondingly equal to $Mod_D = 26.5$ kBq/m² and $Mod_W = 199$ kBq/m² and are shown in the figure by dotted vertical straight lines. However, this is a mixture of only two distributions (15) describing a distribution of mean values, x_o, for the sub-sites.

Figure 8 shows the clouds of points (x_{oi}, s_i) for dry (triangles) and wet (circles) fallouts corresponding to selected functions (15) and coefficients of variation (13) included in the interval [0.350, 0.514]. This interval is selected as an example and corresponds to the experimental values of coefficients of variation for sub-sites P4.1-4.4. Contamination of the i^{th} sub-site is described by a lognormal distribution $\Lambda_i(x|\mu_i, \sigma_i^2)$ whose parameters can be determined by simulation, as in the example given in 4.4.1.

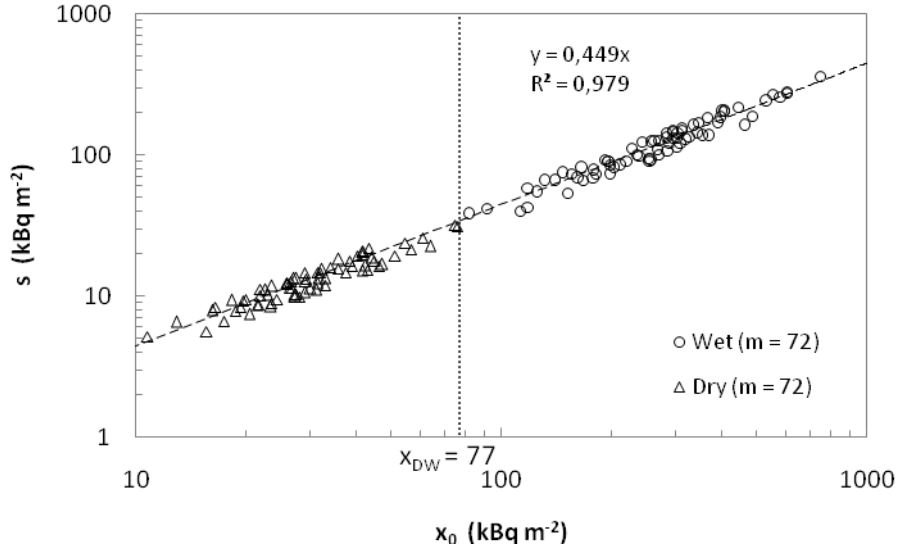

Figure 8. Clouds of points (x_{oi}, s_i) for dry and wet fallouts.

The derived mixtures (8) for the activity density distributions, x, of the dry and wet fallouts are shown in Figure 9 and in Figure 10 by heavy grey curves. Dashed lines show the results of the fitting of lognormal distributions to these mixtures. The derived mixtures are adequately described by lognormal distributions. The distribution of the activity density in the entire site, including both zones (dry and wet fallouts), is described by mixtures of the two mixtures shown in Figure 11 by the heavy grey line. As observed, unlike the mixture of two distributions (15), this mixture proved to be unimodal. Moreover, this mixture can be roughly described by the lognormal distribution. Fitting of the lognormal distribution to the mixture is shown in Figure 11 by the dashed line.

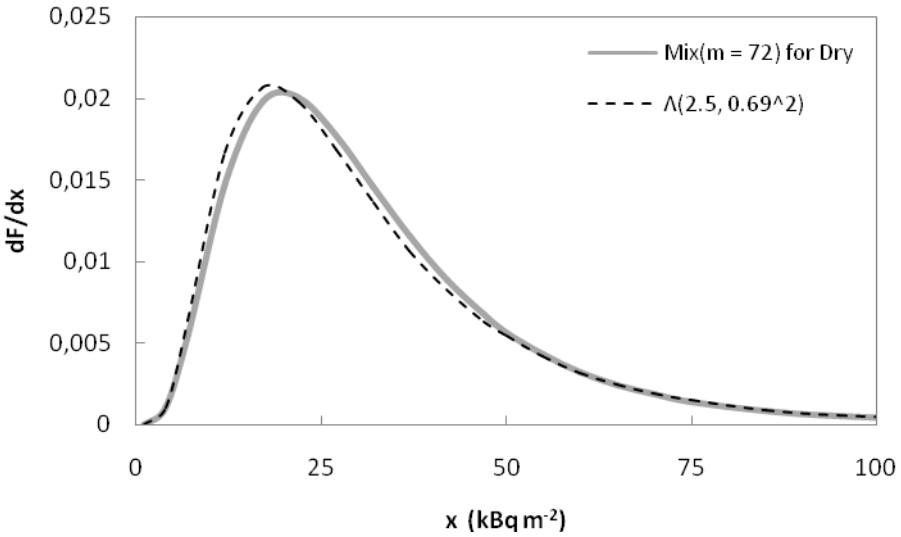

Figure 9. Fitting of lognormal distribution to mixture for dry fallout.

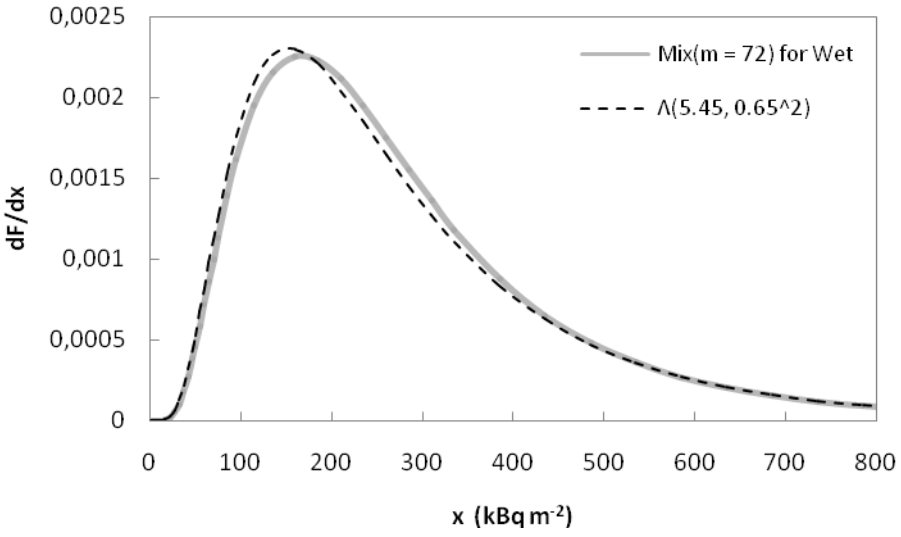

Figure 10. Fitting of lognormal distribution to mixture for wet fallout.

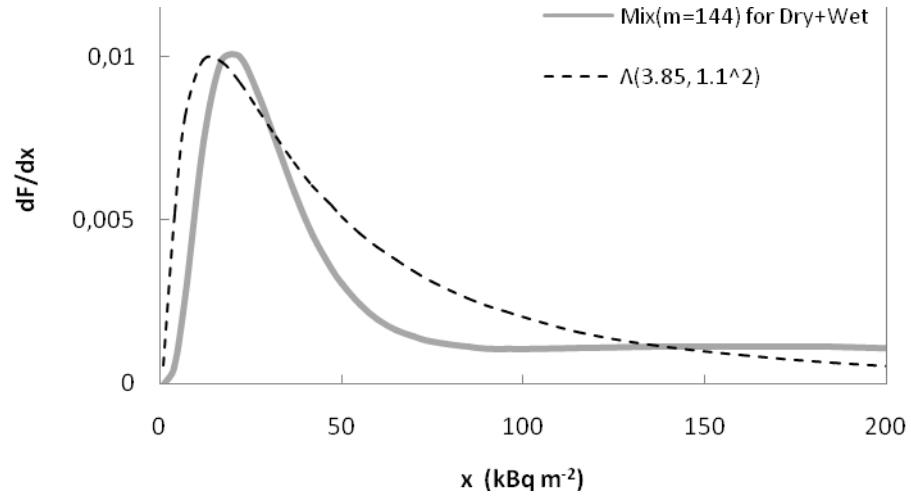

Figure 11. Fitting of lognormal distribution to mixture for dry and wet fallouts.

Attention should be paid to the following important factor. One can show that the derived mixture of two mixtures for dry and wet fallouts turned out to be unimodal only by virtue of the intuitively obvious condition that was used in plotting the point clouds in Figure 8, and according to which point clouds (s_i, x_{oi}) for dry and wet fallouts should be actually into contact with each other.

In Figure 8, the boundary between clouds corresponds to the dotted line x_{DW} = 77 kBq/m². The following consideration can be given in favour of this condition. On the diagram (map) of radioactive contamination to boundaries between zones with dry and wet fallouts (for example, boundaries shown in Figure 1b), some isoline $x_o = x_{DW}$ will correspond. Due to this, in a figure such as the Figure 8, the clouds (s_i, x_{oi}) should be spaced on both sides of graph of equation $x_o = x_{DW}$.

Here, only a simulated example is given. Still, it shows that if the deposition structure is based on the lognormality of the local contamination regions, then the parameters of the lognormal distribution describing dry and wet fallouts the same territory are not absolutely independent. In the example considered here, the intuitively obvious condition of neighbourhood of point clouds (s_i, x_{oi}) for dry and wet fallouts was used (in other words, the boundary conditions provide interconnections of both distributions).

For deeper analysis of the distribution describing dry and wet fallouts, it is necessary to use experimental data derived separately for each type of fallout on the same territory as a result of some critical event. It should be from one, and not several events. Indeed, in the case of deposition formed by varied critical events, the clouds of point (s_i, x_{oi}) in Figure 8 may be spaced along the abscissa axis at considerable remoteness from each other. In this case the mixture of lognormal distributions (8) may have two maxima (not be unimodal).

The data analysis for the Chernobyl and Fukushima fallouts given in [2] shows that the statistical properties of deposition considered above also hold for the activity concentration quantity (Bq/kg). In this case scattering of points (x_o, s) is shown in Figure 12. The plots also cite data for Fukushima fallouts (grey squares) corresponding to 63rd and 64th datasets of Table 1b in [2].

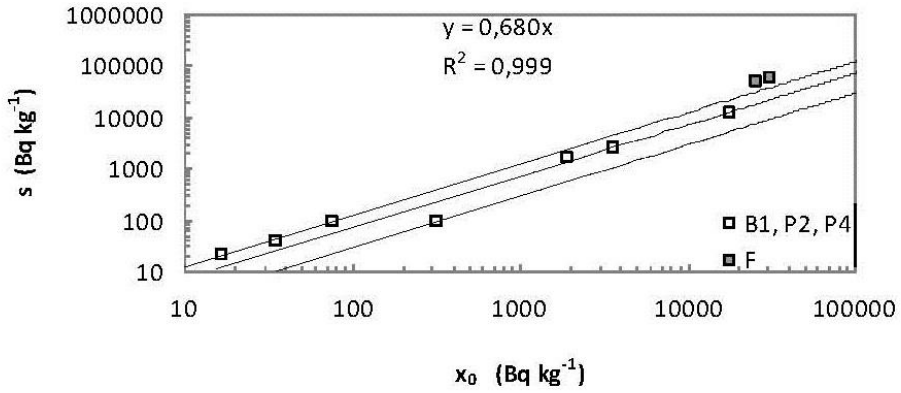

Figure 12. Values of standard deviation, s, against sample mean, x_0, for data in Table 1b in [2].

Conclusions

Pollution of individual sites and their aggregations can be described by a family of lognormal distributions by virtue of certain statistical and structural properties inherent in spatial patterns of radionuclide deposition, namely,

1) The spatial deposition pattern has mosaic structure whose elements are tiny areas with contamination described by lognormal distributions.

2) Regression dependence of the coefficient of variation from the mean is not.

3) In the case of the division of an arbitrary site/territory into a multiplicity of equidimensional sub-sites ($m >> 1$) the following regularities are valid:

— The mean values of the sub-sites' contamination are distributed lognormally (see (15)).

— The coefficients of variation for the sub-sites are randomly distributed in some interval of values which, in turn, is included in the interval $[CV_{min}, CV_{max}]$, where $CV_{min} \approx 0.2$, $CV_{max} \approx 0.9$, at least for areas of sub-sites from $1.56 \cdot 10^{-6}$ km² to 142 km² (see (11), (12)).

4) The probability of describing a dataset with a lognormal distribution goes up with an increased sample size. Datasets with a sampling size $n \geq 100$ are described, as a rule, by lognormal distributions.

Finally, the statistical and structural properties of radionuclide deposition are not related to the phenomenon of radioactivity. Consequently, the key results and conclusions of this article are applicable to non-radioactive deposition formed by short-term fallout, similar to Chernobyl and Fukushima.

References:

1. Daniels, W.M., Higgins, N.A., 2002. Environmental Distribution and the Practical Utilisation of Detection Limited Environmental Measurement Data.NRPB-W13. ISBN 0 85951 484 6.

2. Grubich, A., Makarevich, V.I., Zukova O.M., 2013. Description of spatial patterns of radionuclide deposition by lognormal distribution and hot spots.J.Environ.Radioact.126, 264–272.

3. Raes, F., De Cort, M., Graziani, G., 1991.Multi-fractal nature of radioactivity deposition on soil after the Chernobyl accident. Health Phys. 61, 271–274.

4. De Cort, M., Dubois, G., Fridman, Sh.D., Germenchuk, M.G., Izrael, Yu.A., Janssens, A., Jones, A.R., Kelly, G.N., Kvasnikova, E.V., Matveenko, I.I., Nazarov, I.M., Pokumeiko, Yu.M., Sitak, V.A., Stukin, E.D., Tabachny, L.Ya., Tsaturov, Yu.S., Avdyushin, S.I., 1998. Atlas of Caesium Deposition on Europe after the Chernobyl Accident. EUR Report 16733. Office for Official Publications of the European Communities, Luxembourg.

5. Grubich, A.O., 2012. Multifractal structure of the ^{137}Cs fallout at small spatial scales. J. Environ. Radioact.107, 51–55.

6. Aitchison, J., Brown, J.A.C., 1957. The Lognormal Distribution.University Printing House, Cambridge.